



## **Three-Dimensional Nuclear Assessment for the Chamber of Z-Pinch Power Plant**

**M. Sawan, L. El-Guebaly, P. Wilson**

**November 2006**

**UWFDM-1312**

Presented at the 17th ANS Topical Meeting on Fusion Energy, 13-15 November 2006, Albuquerque NM; published in *Fusion Science and Technology*, 52/4 (November 2007) 763-770.

***FUSION TECHNOLOGY INSTITUTE***

***UNIVERSITY OF WISCONSIN***

***MADISON WISCONSIN***

### **DISCLAIMER**

This report was prepared as an account of work sponsored by an agency of the United States Government. Neither the United States Government, nor any agency thereof, nor any of their employees, makes any warranty, express or implied, or assumes any legal liability or responsibility for the accuracy, completeness, or usefulness of any information, apparatus, product, or process disclosed, or represents that its use would not infringe privately owned rights. Reference herein to any specific commercial product, process, or service by trade name, trademark, manufacturer, or otherwise, does not necessarily constitute or imply its endorsement, recommendation, or favoring by the United States Government or any agency thereof. The views and opinions of authors expressed herein do not necessarily state or reflect those of the United States Government or any agency thereof.

# **Three-Dimensional Nuclear Assessment for the Chamber of Z-Pinch Power Plant**

M. Sawan, L. El-Guebaly, P. Wilson

Fusion Technology Institute  
University of Wisconsin  
1500 Engineering Drive  
Madison, WI 53706

<http://fti.neep.wisc.edu>

November 2006

UWFDM-1312

Presented at the 17th ANS Topical Meeting on Fusion Energy, 13-15 November 2006, Albuquerque NM; published in *Fusion Science and Technology*, 52/4 (November 2007) 763-770.

# THREE-DIMENSIONAL NUCLEAR ASSESSMENT FOR THE CHAMBER OF Z-PINCH POWER PLANT

M. Sawan, L. El-Guebaly, and P. Wilson

Fusion Technology Institute, University of Wisconsin, Madison, WI, [sawan@engr.wisc.edu](mailto:sawan@engr.wisc.edu)

Detailed three-dimensional nuclear analyses have been carried out for the chamber of a power plant concept that utilizes the Z-Pinch driven inertial confinement technology with a target yield of 3 GJ and repetition rate of 0.1 Hz per chamber. The elliptical chamber concept was modeled with the double-layered Recyclable Transmission Lines (RTL). Thick liquid jets are utilized to breed tritium, absorb energy, and shield the chamber wall. Two liquid breeder options were considered; the molten salt *Flibe* and the *LiPb* eutectic ( $Li_{17}Pb_{83}$ ). The chamber wall is made of the low activation ferritic steel alloy F82H. While both breeders have the potential for achieving tritium self-sufficiency, the thermal power is ~6.5% higher with *LiPb*. However, a 55% thicker jet zone is required with *LiPb* to provide adequate chamber wall shielding. A thicker chamber wall is required with *LiPb* to reduce the nuclear energy leakage below 1%. The chamber wall does not need replacement except for the top part around the jet nozzles. Helium production in the chamber wall protected by *LiPb* is much lower than that with *Flibe*. Rewelding is possible only in the lower part of chamber wall below the pool.

## I. INTRODUCTION

The Z-Pinch Power Plant is the first concept to use the results at Sandia National Laboratories' Z accelerator

in a power plant application.<sup>1-3</sup> The Z accelerator using x-rays from plasma being pinched on the z-axis of the pulsed power driver can be used to indirectly heat an inertial confinement fusion capsule. An initial Z-Pinch Power Plant named ZP3 was developed on the basis of a 1000 MW electrical output plant scale. To achieve this power level, multiple chambers or units will be required.

The present strategy for Z-Pinch IFE is to use high-yield targets (~3 GJ/shot) and low repetition rate per chamber (~0.1 Hz). The present mainline choice for a Z-Pinch IFE power plant uses an LTD (Linear Transformer Driver) repetitive pulsed power driver, a Recyclable Transmission Line (RTL), a dynamic hohlraum Z-Pinch-driven target, and a thick-liquid wall chamber as shown in Fig. 1.<sup>4</sup> Thick-liquid walls have been used in previous inertial fusion designs.<sup>5</sup> The chamber pressure is 10-20 Torr of an inert gas such as Ar. The RTL connects the pulsed power driver directly to the Z-Pinch-driven target, and is made from frozen coolant or a material that is easily separable from the coolant (such as low activation ferritic steel). The RTL/target assembly is inserted through a single opening at the top of the thick liquid wall power plant chamber. The RTL is destroyed by the fusion explosion, but the RTL materials are recycled,<sup>6</sup> and a new RTL is inserted before each shot.

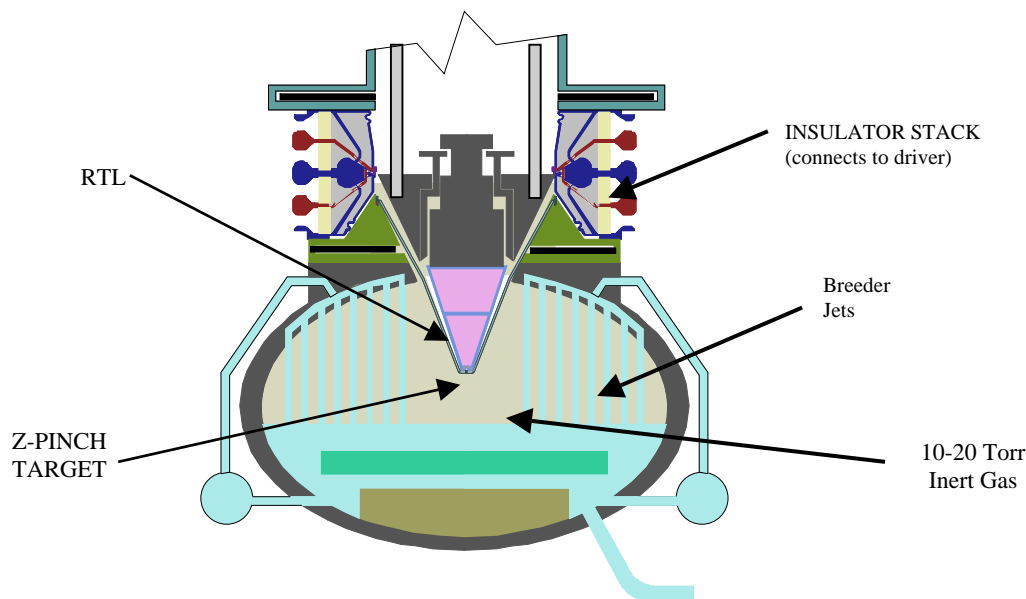


Fig. 1. Elliptical Z-Pinch IFE chamber concept.

An effective system design for the plant requires an integrated blanket that absorbs the fusion neutron energy, breeds tritium to fuel the targets, shields the structural wall from neutron damage, and mitigates the shock to protect the structural wall. Two candidate liquid breeder/coolant materials were considered.<sup>7</sup> These are the molten salt Flibe ( $F_4Li_2Be$ ) and the  $Li_{17}Pb_{83}$  eutectic. In this paper, detailed three-dimensional (3-D) nuclear analysis is presented for the chamber to assess the nuclear performance with the two liquid breeder options.

## II. CALCULATION PROCEDURE

Preceding the 3-D analysis, a series of parametric one-dimensional (1-D) analysis was established to guide the design process and identify the initial configuration for the 3-D analysis.

### II.A 1-D Parametric Analysis

The 1-D spherical model included the essential elements that impact the nuclear parameters: the details of the target at burn, thin layer of the RTL, breeder jets (100% dense) at 1 m from target center, and chamber wall. The variable-size gap behind the jets was eliminated to help estimate the peak radiation damage at the chamber wall. The DANTSYS code<sup>8</sup> was used along with the FENDL-2 data library in 175 neutron and 42 gamma group structure with the  $P_3-S_8$  approximation.

The sensitivity of TBR, dpa, He production, and heat leakage to the thickness of the candidate breeders ( $F_4Li_2Be$  and  $Li_{17}Pb_{83}$ ) was examined. Figures 2-6 display the results and the following observations can be made:

Figures 2 and 3:

- 42 cm Flibe ( $F_4Li_2Be$ , 100% dense with natural enrichment) protects the wall for plant life (dpa = 200) and over-breeds tritium (TBR > 1.1).
- 80 cm  $Li_{17}Pb_{83}$  (100% dense with natural enrichment) meets the breeding requirement (TBR = 1.1) and protects the wall for plant life (dpa = 200).

Figure 4:

- No significant change in breeding with Flibe enrichment.
- LiPb enrichment increases breeding significantly and reduces wall damage (not shown in Fig. 4).
- 3-D analysis should determine reference breeder thickness and enrichment.

Figure 5:

- Chamber wall cannot be rewelded at any time during operation (He production  $\gg$  1 He appm).
- Mechanical attachments or other means should be considered for wall assembly particularly behind the jets.

Figure 6:

- 42 cm Flibe (100% dense) and 30 cm wall/shield recover 99% of total nuclear heating.
- 80 cm LiPb and 50 cm wall/shield recover 99% of total nuclear heating.

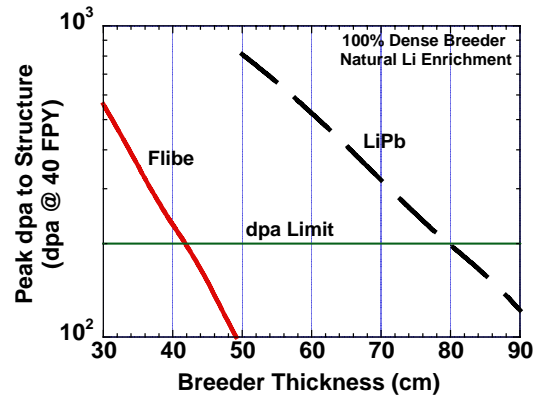


Fig. 2. Variation of dpa at chamber wall with breeder thickness.

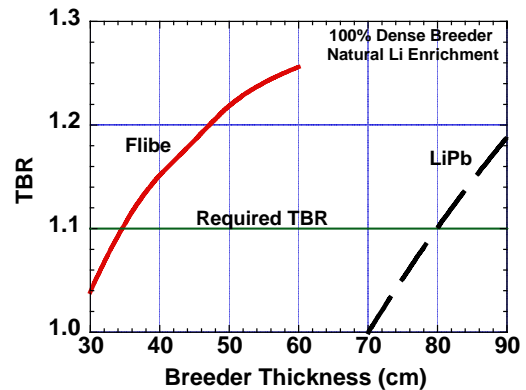


Fig. 3. The increase in TBR with breeder thickness.

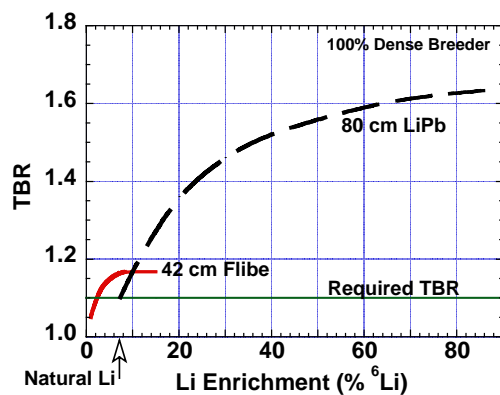


Fig. 4. TBR versus Li enrichment.

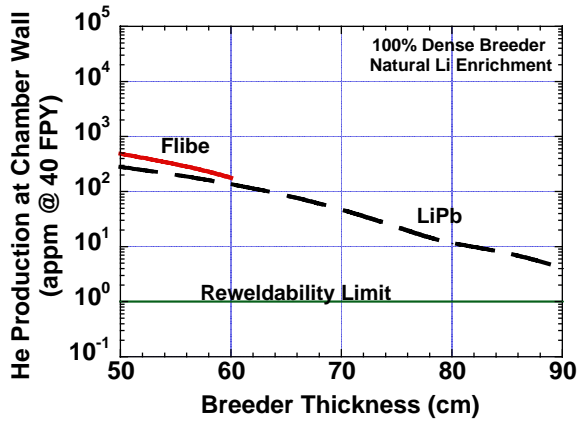


Fig. 5. Sensitivity of He production at chamber wall to breeder thickness.

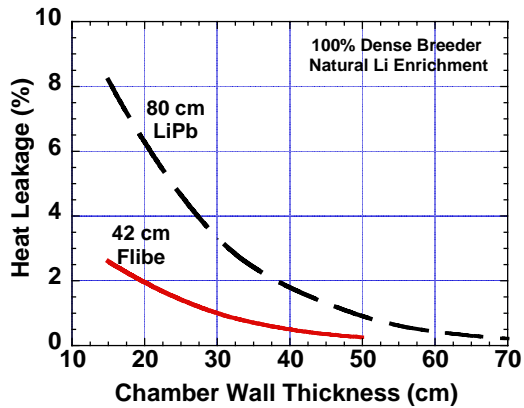


Fig. 6. The reduction of heat leakage with chamber wall thickness.

This concludes the 1-D scoping assessment. In the following section, the 3-D analysis will call for measures to enhance the engineering aspect of the design based on the overall nuclear performance. Optimization of the jet dimensions and breeder parameters, definition of the heat load to individual components, and characterization of the radiation damage profile were given considerable attention during the 3-D study.

## II.B 3-D Analysis

Detailed 3-D neutronics calculations have been performed for the chamber using the latest version of the continuous energy, coupled neutron-gamma Monte Carlo code MCNP,<sup>10</sup> version 5 along with nuclear data based on the most recently released evaluation FENDL-2.1.<sup>11</sup> The elliptical chamber concept shown in Fig. 1 was modeled. The chamber has an inner diameter of 10 m and a height of 6 m. The double-layered RTL is made of carbon steel. The layers were modeled as two truncated cones with the

outer layer being 0.9 mm thick and the inner layer having a thickness of 0.5 mm. A 10 mm gap exists between the two RTL layers. The imploded target radial build and composition with a  $\rho R$  of 3 was included in the model at the lower tip of the RTL. The target is located at 0.5 m above the chamber geometrical center. The target configuration at ignition was modeled by a set of spherical shells. The compressed DT core has a radius of 0.57 mm and is surrounded by 8.3 mm thick Be, 0.11 mm thick CH, and 1.65 mm thick Au shells.<sup>9</sup> 14.1 MeV source neutrons were sampled uniformly from the DT spherical core.

The liquid jets and pool breed the tritium required to fuel the targets, absorb the energy carried by neutrons, x-rays, and ion debris emitted from the target, and shield the structural chamber wall from neutron damage. We performed the 3-D calculations for the two liquid breeder options considered. Figure 7 gives the 3-D geometrical model used for the chamber that utilizes the molten salt Flibe as the breeding liquid. The jet zone has an inner radius of 1 m. Eight rows of Flibe jets are utilized with the outer surface of the last row at a radius of 2.1 m. The packing fraction of the jets is 37%. The pool surface is 1 m below the chamber center implying that the maximum pool depth is 2 m. Gas is bubbled in the pool for shock mitigation. A density factor of 0.8 is used for the Flibe in the pool. Flibe foam at 0.1 density factor is used to fill the RTL cone. Natural lithium is used in the Flibe. The chamber wall is 0.3 m thick and is made of the low activation ferritic steel alloy F82H.<sup>7,12</sup> The nozzle zone of the chamber wall above the Flibe jets consists of 66% F82H and 34% Flibe. The insulator stack above the chamber is simulated in the 3-D model by a zone made of epoxy to evaluate the expected insulator radiation environment.

For the chamber that utilizes the lithium lead eutectic ( $\text{Li}_{17}\text{Pb}_{83}$ ) as the breeding liquid, a thicker jet zone is needed to provide adequate shielding for the chamber wall. Twelve rows of jets are used with the surface of the outer row at a radius of 2.7 m. The lithium is slightly enriched to 20% Li-6. The chamber wall thickness is increased to 0.5 m to reduce the energy leakage from the chamber. LiPb foam with 0.1 density factor is used inside the RTL cone. Several splitting surfaces have been added to allow for utilizing the geometry splitting with Russian Roulette variance reduction techniques<sup>10</sup> needed to reduce the statistical uncertainties in the calculated nuclear parameters. The calculations have been performed with 100,000 source particles yielding statistical uncertainties less than 0.5% in integral quantities and 2% in local parameters. The results were normalized to a fusion power of 300 MW per chamber (DT target yield of 3 GJ and repetition rate of 0.1 Hz).

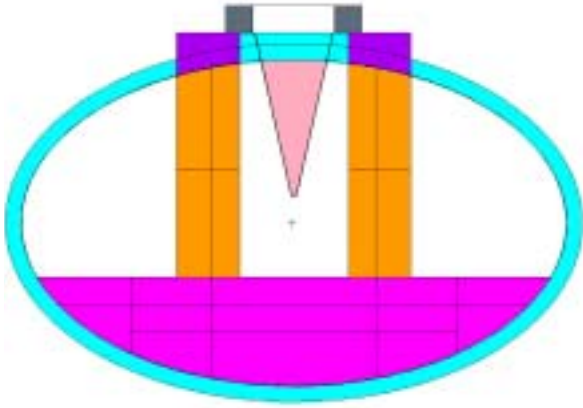


Fig. 7. The MCNP 3-D model for the chamber with Flibe liquid breeder.

### III. TRITIUM BREEDING

Tritium production in the different breeder zones of the chamber was determined for the two breeder options. The results are given in Table I. It is clear that most of the tritium breeding occurs in the jet zone although the amount of breeder in the jets is much smaller than that in the pool. The reason is that the jets are exposed to 88% of the source neutrons emanating from the target while the pool is exposed directly to only 9% of the source neutrons. The overall tritium breeding ratio (TBR) is  $>1.1$  in both cases implying that both breeder options have the potential for achieving tritium self-sufficiency.

TABLE I. Tritium Production in the Different Breeder Zones of the Chamber

	Tritium Production per Fusion	
	Flibe Breeder	LiPb Breeder
Jets	0.840	0.711
Nozzle Zone	0.019	0.053
Pool	0.246	0.362
RTL Foam	0.011	0.005
Overall TBR	1.116	1.131

### IV. NUCLEAR HEATING

Nuclear energy deposited by neutrons and gamma photons in the chamber components was determined for the two designs with Flibe and LiPb. Table II lists the amount of nuclear heating in the target layers for the 3 GJ DT yield shot. These results were found to be independent of the breeder choice. Adding the amount of nuclear heating in the target to the 3.5 MeV carried by the alpha particle from the fusion reaction implies that the total energy carried by x-rays and ion debris per DT fusion is 4.987 MeV. These results indicate that out of the 3 GJ DT

target yield 2.147 GJ is carried by neutrons and 0.853 GJ is carried by x-rays and ion debris.

TABLE II. Nuclear Heating in Target Layers

	MeV/fusion	MJ per 3GJ DT yield shot
DT core	1.476	251.59
Be shell	$9.62 \times 10^{-3}$	1.64
CH shell	$2.95 \times 10^{-4}$	0.05
Au shell	$4.13 \times 10^{-4}$	0.07
TOTAL	1.487	253.35

Table III gives the breakdown of the amount of nuclear heating deposited in the chamber components for each 3 GJ yield shot with the Flibe breeder. The values of surface heating deposited by x-rays and ion debris at component surfaces facing the target are also given as well as the total thermal energy in each of the chamber components. The overall energy multiplication defined as the ratio of the total thermal power to the fusion power is 1.115. The results for the chamber with LiPb breeder are given in Table IV. The overall energy multiplication in this case is 1.187 which is  $\sim 6.5\%$  higher than that with Flibe.

TABLE III. Nuclear Heating and Total Thermal Energy in Flibe Chamber Components

	Nuclear Heating (GJ/shot)	X&D Heating (GJ/shot)	Thermal Energy (GJ/shot)
Jets	1.798	0.748	2.546
Pool	0.402	0.072	0.474
Chamber Wall	0.139	0.000	0.139
Nozzle Zone	0.062	0.000	0.062
RTL Support Structure	0.054	0.020	0.074
RTL	0.008	0.010	0.018
RTL Foam	0.033	0.000	0.033
Total	2.496	0.850	3.346

TABLE IV. Nuclear Heating and Total Thermal Energy in LiPb Chamber Components

	Nuclear Heating (GJ/shot)	X&D Heating (GJ/shot)	Thermal Energy (GJ/shot)
Jets	1.624	0.748	2.372
Pool	0.494	0.072	0.566
Chamber Wall	0.320	0.000	0.320
Nozzle Zone	0.158	0.000	0.158
RTL Support Structure	0.084	0.020	0.104
RTL	0.007	0.010	0.017
RTL Foam	0.023	0.000	0.023
Total	2.710	0.850	3.560

The pulsed nature of inertial fusion leads to sudden energy deposition in the liquid resulting in instant pressurization and disassembly with possible high speed acceleration of fluid masses inside the chamber. This phenomenon is referred to as isochoric heating. To help assess the problem we determined the distribution of energy deposition per unit volume of the fluid surrounding the target during each pulse. The results are shown in Figs. 8 and 9 for Flibe and LiPb, respectively.

Flibe has higher nuclear heating per unit volume at the front zones but lower values at the back zones compared to LiPb. The mesh tally capability of MCNP5 was used to calculate the detailed distribution (5 cm x 5 cm mesh) of the isochoric heating in the Flibe jets (Fig. 10). The lower values close to target are due to added attenuation in the RTL component near the target.

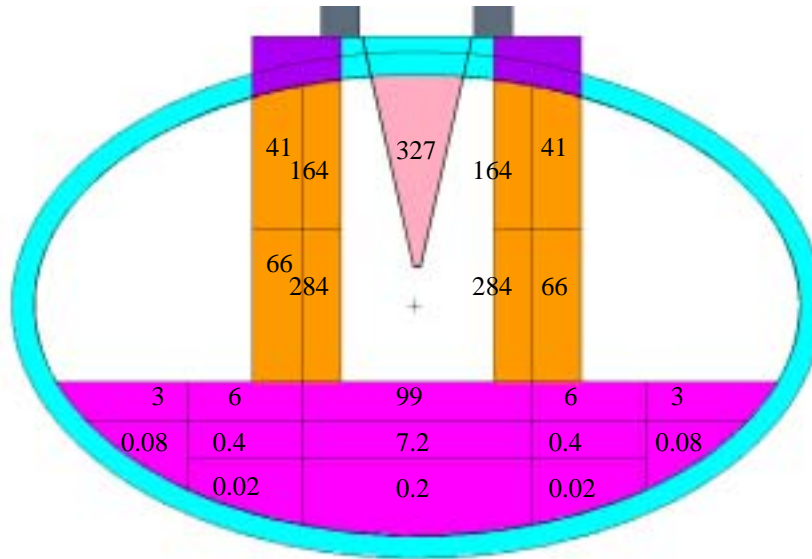


Fig. 8. Volumetric heating per shot ( $J/cm^3$ ) in Flibe.

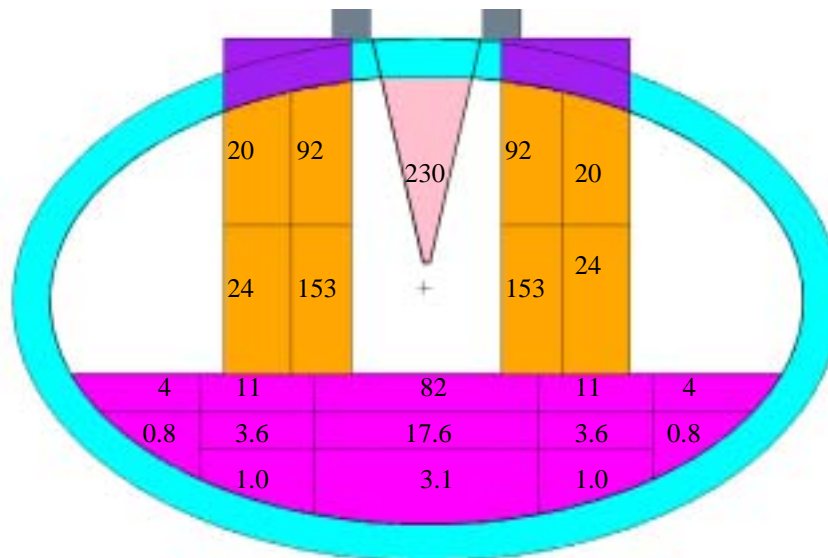


Fig. 9. Volumetric heating per shot ( $J/cm^3$ ) in LiPb.

## V. RADIATION DAMAGE IN CHAMBER WALL

3-D neutronics calculations were performed to determine the variation of damage rate at the inner surface

of the chamber wall for both designs with Flibe and LiPb breeders. Figure 11 gives the cumulative dpa rate along the inner surface of the chamber starting from the bottom of the pool and ending at the top of the chamber behind

the RTL. A plant lifetime of 40 full power years (FPY) was assumed. The results for chambers with Flibe and LiPb are included for comparison. Radiation damage in the chamber wall is about a factor of 2 higher with LiPb. The largest chamber damage occurs at the unshielded area between the RTL and the jets. Based on a lifetime radiation damage limit of 200 dpa, the chamber wall is expected to be a lifetime component except for the top part starting in the nozzle zone. The nozzle zone of the chamber wall should be replaced once in the case of Flibe or three times in the LiPb design. The RTL support structure needs to be replaced a factor of ~2 more frequently. Figure 12 is a schematic that illustrates the lifetime for the different chamber regions for both the Flibe and LiPb designs.

To assess the reweldability of the chamber wall, we determined the cumulative helium production at the inner surface of the chamber wall. The results are shown in Fig. 13 for the two breeder options. Helium production in the chamber wall is lower with LiPb. Based on a rewelding limit of 1 He appm, the part of the chamber wall below the LiPb pool is reweldable. On the other hand, with Flibe, only the part of the chamber wall that is ~20 cm below the pool surface can be rewelded. Hence, although most of the chamber wall is lifetime component, rewelding is allowed only in a small part below the breeder pool.

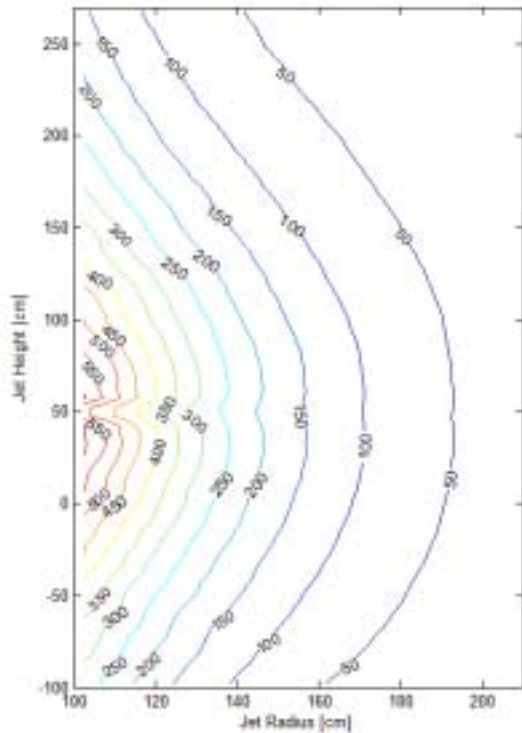


Fig 10. Detailed spatial distribution of jet volumetric heating ( $J/cm^3$ ) in Flibe jet.

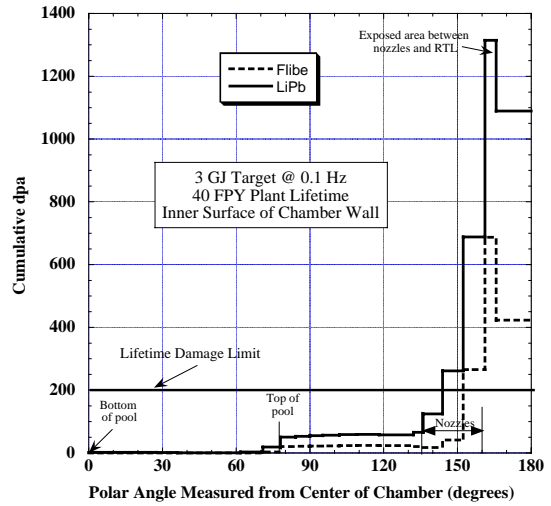


Fig. 11. Variation of cumulative radiation damage at inner surface of chamber wall.

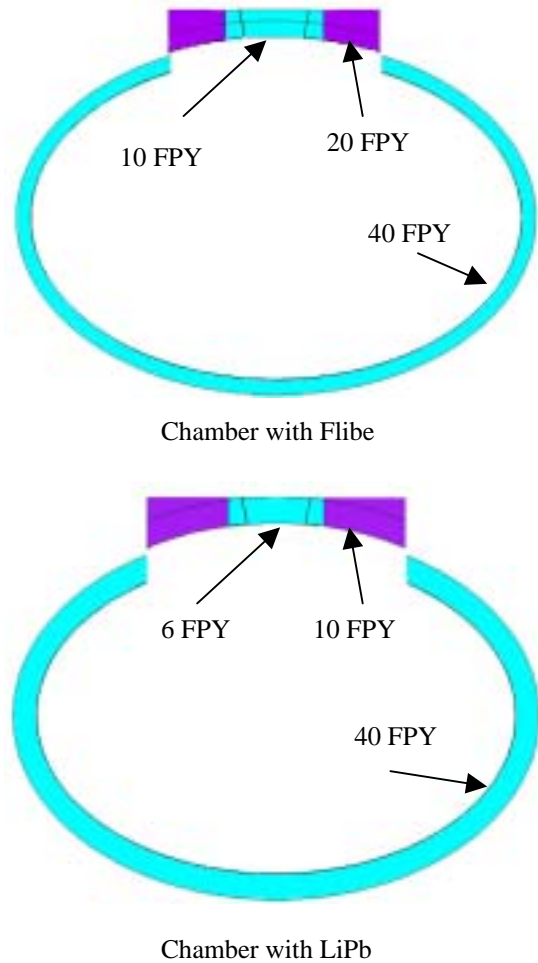


Fig. 12. Lifetime of chamber zones.

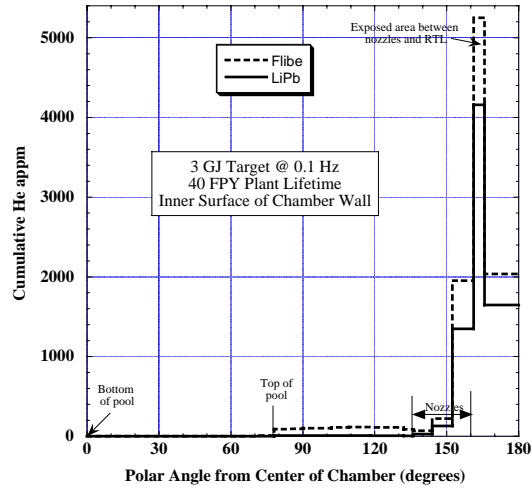


Fig. 13. Variation of cumulative helium production at inner surface of chamber wall.

## VI. INSULATOR SHIELDING

As shown in Fig. 1, an insulator stack is located at the interface between the pulsed power driver and the coax conical RTL system. We calculated the absorbed dose and fast neutron ( $E > 0.1$  MeV) fluence in the insulator stack located above the chamber with both Flibe and LiPb breeders. Performance of the insulators is very sensitive to radiation damage. The mechanical properties of organic insulators (epoxies and polyimides) degrade at absorbed doses larger than  $10^9$ - $10^{10}$  Rads.<sup>13</sup> Ceramic insulators are 2-3 orders of magnitude more radiation resistant than organic insulators. Candidate materials include  $Al_2O_3$ , MgO, and spinel ( $MgAl_2O_4$ ). Spinel offers the lowest mechanical and structural degradation in a nuclear environment among its class of solid ceramic insulators. The fluence limit for ceramics is determined only by the maximum swelling to be tolerated. A maximum swelling of 3% is considered. This corresponds to fast neutron ( $E > 0.1$  MeV) fluences of  $1.1 \times 10^{22}$  and  $4 \times 10^{22}$  n/cm<sup>2</sup> for MgO and spinel, respectively.<sup>14</sup> Table V lists the end-of-life organic insulator absorbed dose and fast neutron fluence for the chamber designs with Flibe and LiPb. Using LiPb results in about a factor of 5 higher insulator radiation levels. The absorbed dose in organic insulators is excessive and should not be used at these locations. On the other hand, if ceramic insulators are used, they are expected to survive for the whole plant lifetime.

TABLE V. Absorbed Dose and Fast Neutron Fluence in the Insulator After 40 FPY

	Flibe	LiPb
End-of-life organic insulator dose (Rads)	$4.4 \times 10^{12}$	$2.0 \times 10^{13}$
End-of-life fast neutron fluence (n/cm <sup>2</sup> )	$1.4 \times 10^{21}$	$6.4 \times 10^{21}$

## VII. SUMMARY AND CONCLUSIONS

The 3-D neutronics calculations for the Z-Pinch power plant chamber indicate that the thermal power is ~6.5% higher when LiPb is used instead of Flibe. However, a 55% thicker jet zone is required with LiPb to provide adequate chamber wall shielding. A low lithium enrichment (20% <sup>6</sup>Li) in LiPb is adequate for tritium self-sufficiency. Both breeder options have the potential for achieving tritium self-sufficiency. Lithium enrichment can be used as a knob for adjusting the TBR if needed. A thicker chamber wall is required with LiPb to reduce nuclear energy leakage to <1%. Radiation damage in the chamber wall is a factor of ~2 higher with LiPb. In both cases, the chamber wall does not need replacement except for the top including part of the nozzle zone. He production in the chamber wall protected by LiPb is much lower than that with Flibe. Rewelding is possible only in the lower part of chamber wall below the pool. About a factor of 5 higher insulator radiation levels result with LiPb. Organic insulators cannot be used but ceramic insulators will survive for the whole plant lifetime of 40 FPY.

## ACKNOWLEDGMENTS

The work was performed under the auspices of the Sandia National Laboratories (contract # 297000).

## REFERENCES

1. C. OLSON, G.E. ROCHAU, S. SLUTZ, et al., "Development Path for Z-Pinch IFE," *Fusion Science and Technology*, **47**, 633 (2005).
2. G.E. ROCHAU AND C. MORROW, "A Concept for a Z-Pinch Fusion Power Plant," SAND2004-1180, Sandia National Laboratories (March 2004).
3. G.E. ROCHAU AND C. MORROW, "A Concept for Containing Inertial Fusion Pulses in a Z-Pinch Driven Power Plant," *Fusion Science and Technology*, **43**, 447 (2003).
4. C.L. OLSON et al., "Z-Pinch IFE Program Final Report for FY05," Sandia National Laboratories report, SAND Report, to be published in 2006.
5. R.W. MOIR, R.L. BIERI, X.M. CHEN et al., "HYLIFE-II: A Molten-Salt Inertial Fusion Energy Power Plant Design-Final Report," *Fusion Technology*, **25**, 5 (1994).
6. L. EL-GUEBALY, P. WISON, and M. SAWAN, "Activation and Waste Stream Analysis for RTL of Z-Pinch Power Plant," *Fusion Science and Technology*, this issue.
7. L. EL-GUEBALY, M. SAWAN, I. SVIATOSLAVSKY et al., "Z-Pinch Chamber Assessment and Design," *Fusion Science and Technology*, this issue.

8. R.E. ALCOUFFE, R. BAKER, F. BRINKLEY, et al., "DANTSYS 3.0, A Diffusion Accelerated Neutral Particle Transport Code System," LA-12969-M, Los Alamos National Laboratory (June 1995).
9. G. MOSES, University of Wisconsin-Madison, private communication (June 2005).
10. X-5 Monte Carlo Team, "MCNP-A General Monte Carlo N-Particle Transport Code, Version 5-Volume II: Users Guide," LA-CP-03-0245, Los Alamos National Laboratory (April 2003).
11. D.L. ALDAMA AND A. TRKOV, "FENDL-2.1, Update of an Evaluated Nuclear Data Library for Fusion Applications," Report INDC(NDS)-467, International Atomic Energy Agency (2004).
12. S. ZINKLE, J. ROBERTSON, AND R. KLUEH, "Thermophysical and Mechanical Properties of Fe-(8-9)%Cr Reduced Activation Steels," Fusion Materials Semiannual Progress Report for the Period Ending June 30, 2000 (DOE/ER-0313/28), pp. 135-143 (2000).
13. M. SAWAN AND P. WALSTROM, "Superconducting Magnet Radiation Effects in Fusion Reactors," *Fusion Technology*, **10/3**, 741 (1986).
14. G. HURLEY et al., "Structural Properties of MgO and MgAl<sub>2</sub>O<sub>4</sub> After Fission Neutron Irradiation Near Room Temperature," LA-UR 81-2078, Los Alamos National Laboratory (1981).